MCB
Journals.ASM.org

Mextli Is a Novel Eukaryotic Translation Initiation Factor 4E-Binding Protein That Promotes Translation in *Drosophila melanogaster*

Greco Hernández,[a,b]* Mathieu Miron,[b] Hong Han,[a] Niankun Liu,[a] Jérémy Magescas,[a] Gritta Tettweiler,[a] Filipp Frank,[b] Nadeem Siddiqui,[b] Nahum Sonenberg,[b] Paul Lasko[a]

Department of Biology, McGill University, Montreal, Quebec, Canada[a]; Department of Biochemistry and Goodman Cancer Research Center, McGill University, Montreal, Quebec, Canada[b]

Translation is a fundamental step in gene expression, and translational control is exerted in many developmental processes. Most eukaryotic mRNAs are translated by a cap-dependent mechanism, which requires recognition of the 5′-cap structure of the mRNA by eukaryotic translation initiation factor 4E (eIF4E). eIF4E activity is controlled by eIF4E-binding proteins (4E-BPs), which by competing with eIF4G for eIF4E binding act as translational repressors. Here, we report the discovery of Mextli (Mxt), a novel *Drosophila melanogaster* 4E-BP that in sharp contrast to other 4E-BPs, has a modular structure, binds RNA, eIF3, and several eIF4Es, and promotes translation. Mxt is expressed at high levels in ovarian germ line stem cells (GSCs) and early-stage cystocytes, as is eIF4E-1, and we demonstrate the two proteins interact in these cells. Phenotypic analysis of *mxt* mutants indicates a role for Mxt in germ line stem cell (GSC) maintenance and in early embryogenesis. Our results support the idea that Mxt, like eIF4G, coordinates the assembly of translation initiation complexes, rendering Mxt the first example of evolutionary convergence of eIF4G function.

Translational control plays a prominent role in many cellular and developmental events (1–3). Most eukaryotic mRNAs are translated by a cap-dependent mechanism, whereby the mRNA is recruited to the ribosome through recognition of the 5′-cap structure (m^7GpppN, where N is any nucleotide) by the cap-binding protein eukaryotic translation initiation factor 4E (eIF4E) in a complex (termed eIF4F) with the scaffold protein eIF4G and the RNA helicase eIF4A. eIF4G also interacts with eIF3, which recruits the 43S preinitiation complex (consisting of the 40S ribosomal subunit in association with eIF3, eIF1, eIF1A, and a ternary complex, eIF2-GTP-Met-tRNA^{iMet}) to the 5′ end of the mRNA. eIF4A unwinds the secondary structure in the mRNA 5′ untranslated region (UTR) to allow the small ribosomal subunit to scan along the 5′ UTR to reach the start codon (4, 5).

Due to its crucial role in recruiting mRNAs to the ribosome, eIF4E is a target of several different translational control mechanisms that regulate specific mRNAs, some of which are involved in development, cancer, and synaptic plasticity (2, 5, 6). Numerous eIF4E-binding proteins (4E-BPs), such as Maskin, EAP1, CYFIP1, p20, Cup, and VPg, function as translational repressors by acting as competitive inhibitors of eIF4G binding. Consistent with this, most 4E-BPs share with eIF4G the consensus eIF4E-binding motif YXXXXLϕ (where X is any residue and ϕ is any hydrophobic residue) (2, 5–7).

In *Drosophila*, seven eIF4E isoforms are differentially expressed during development (8), raising the possibility that they are regulated by so-far-unknown 4E-BPs. Here we report the discovery of Mextli (Mxt), a novel 4E-BP. Like eIF4G, Mxt binds eIF3 and several eIF4E isoforms and promotes translation, in sharp contrast to other 4E-BPs that inhibit translation. Mxt contains an MIF4G (middle portion of eIF4G) domain, a canonical hnRNP K homology (KH) RNA-binding domain, and a consensus eIF4E-binding motif. This molecular structure renders Mxt a novel type of modular scaffolding protein that coordinates the assembly of translation initiation complexes that serve as an alternative to eIF4G.

MATERIALS AND METHODS

Bioinformatics. The Jpred3 (9) and HHpred (10) programs were used to search for protein domains. The PSI-BLAST program (11) was used to search for locally similar sequences in protein databases.

Identification of *mextli* and construction of plasmids. Radiolabeled FLAG-HMK-eIF4E-1 was used as a probe to screen a lEx*lox Drosophila* 20- to 22-h embryonic cDNA library (Novagen) by the far-Western method (12). One positive clone expressing 4E-BP (*Thor*) and four positive clones expressing C-terminal fragments of *mxt* were obtained. A full-length cDNA (expressed sequence tag [EST] GH11071) was later obtained (Research Genetics). *mxt* cDNA fragments encoding amino acids (aa) 193 to 314 and aa 553 to 653 were further subcloned into pGEX-3X2C (GE Healthcare) to create expression plasmids. The constructs pDEST17-Mxt and pAWH-Mxt, which encode N-terminal 6×His and C-terminal 3× hemagglutinin (3×HA)-tagged versions of Mxt, were made by subcloning the full-length *mxt* coding region or fragments of it into each vector (Invitrogen and DGRC, respectively). pUASP-Mxt-V5 constructs were made by subcloning C-terminal V5 epitope-tagged versions of the *mxt* full-length open reading frame (ORF) into the vector pUASP-K10 attB (13). The *mxt* cDNA fragment encoding aa 284 to 653 was subcloned into the vector pOAD (14) in frame with the activator domain sequence of GAL4 to generate the construct pAD-Mxt ("prey"). To produce Mxt^{AAA}, the *mxt* sequence TACGATATTGAACACTTGCTC that encodes the eIF4E-binding motif **Y**DIEH**LL** (codons 581 to 587) was mutated to GC CGATATTGAACACGCGGCC, which encodes **A**DIEH**AA** (boldface rep-

Received 8 October 2012 Returned for modification 1 November 2012
Accepted 23 April 2013
Published ahead of print 28 May 2013
Address correspondence to Paul Lasko, paul.lasko@mcgill.ca.
* Present address: Greco Hernández, Division of Basic Research, National Institute of Cancer (Instituto Nacional de Cancerología), Tlalpan, Mexico City, Mexico.
Supplemental material for this article may be found at http://dx.doi.org/10.1128/MCB.01354-12.
Copyright © 2013, American Society for Microbiology. All Rights Reserved.
doi:10.1128/MCB.01354-12

resents highly conserved residues of eIF4E binding domains), using *Pfu* high-fidelity polymerase (Stratagene), and the changes were verified by sequencing.

The constructs pAWH-eIF4E-1, pAWH-eIF4E-6, and pAWH-GFP were made by subcloning the coding regions of eIF4E-1, eIF4E-6, and green fluorescent protein (GFP), respectively, in frame with the C-terminal 3×HA of the vector pAWH. pGEX-FLAG-HMK-4E-1 was generated by cloning the eIF4E-1 coding region in frame with the FLAG-HMK sequence of the plasmid pARDr1, followed by the subcloning of the cassette FLAG-HMK-4E-1 into the vector pGEX6P (Amersham Pharmacia). eIF4E cognate cDNAs (8) were subcloned into the pOBD2 vector (14) in frame with the DNA-binding domain sequence of GAL4 to create the respective pBD-4Es ("bait") plasmids. pMT-4E-HP (CG33100), pMT-Mxc (CG12124), pMT-CBP80 (CG7035), pMT-eIF3a (CG9805), pMT-eIF3c (CG4954), pMT-eIF3e (CG9677), pMT-eIF3f (CG9769), pMT-eIF3h (CG9124), and pMT-CG3225 (CG3225) were created by subcloning the respective coding regions in frame with the V5 epitope into the pMT/V5-His TOPO vector (Invitrogen).

Purification of recombinant Mxt. To purify 6×His-Mxt, the construct pDEST17-Mxt was transformed into the *Escherichia coli* strain BL21-A1 (Invitrogen). Six liters of LB-ampicillin medium was inoculated with a 1/50 concentration of a saturated overnight culture of the transformed bacteria and grown at 37°C to an optical density at 600 nm (OD_{600}) of 0.4. Expression was then induced with 0.2% arabinose, and the temperature was switched to 18°C for 5 h. Bacteria were pelleted and lysed by sonication on ice in 240 ml lysis/washing buffer (50 mM Tris-HCl [pH 8.0], 1 M KCl, 10 mM imidazole, 4 mM β-mercaptoethanol, complete EDTA-free protease inhibitor cocktail [Roche, GmbH], and 1 mM phenylmethylsulfonyl fluoride [PMSF]). Extracts were then spun for 30 min at 10,000 × *g*. Three milliliters of a 50% slurry of Ni-nitrilotriacetic acid (NTA) beads (Qiagen) was added to the supernatant, which was incubated for 2 h at 4°C with slow rotation and then poured into three columns.Each column was then washed four times with 15 ml lysis/washing buffer, and the protein was eluted from each column with 5 ml elution buffer (50 mM NaH_2PO_4 [pH 8.0], 300 mM NaCl, 250 mM imidazole). The protein was dialyzed against Tris-buffered saline (TBS), concentrated in a microfiltration tube to 1 ml, and further purified by fast protein liquid chromatography (FPLC) using a Superdex S200 size exclusion column in fractions of 0.5 ml. The protein was eluted in fractions 2 to 7. Protein was dialyzed immediately against 20 mM HEPES-KOH (pH 7.4) and stored at 4°C for a week.

Generation of antibodies and Western blot analyses. Polyclonal anti-Mextli antibodies were raised in rabbit. Antibody 2101 was made against glutathione *S*-transferase (GST)-Mxt (aa 193 to 314), and antibodies 2103 and 2104 were made against GST-Mxt (aa 553 to 653) fusion proteins. For affinity purification of antibodies, 1 ml of crude serum was first passed through a GST column and then through the appropriate GST-fusion protein column, eluted with 100 mM glycine (pH 3.0), and collected in tubes containing 110 μl of 10× Tris-buffered saline.

Western blot analyses were performed with the following primary antibodies and working dilutions: affinity-purified anti-Mxt 2101, 1:200; affinity-purified anti-Mxt 2103, 1:500; rabbit affinity-purified anti-eIF4E-1 (36530) (15), 1:1,000; rabbit anti-eIF4G (16), 1:2,000; rabbit anti-eIF3b (17), 1:1,000; rabbit affinity-purified anti-eIF4AIII (1192) (18), 1:1,000; rabbit anti-poly(A)-binding protein (PABP) (2482) (19), 1:1,000; rabbit anti-eIF4A (744), 1:3,000; rabbit affinity-purified anti-4E-BP (1868) (20), 1:1,000; affinity-purified rabbit anti-La (21), 1:1,000; mouse monoclonal anti-HA-horseradish peroxidase (HRP) monoclonal antibody (MAb) (3F10; Roche), 1:2,000; mouse monoclonal anti-V5-HRP (Invitrogen), 1:5,000; and mouse monoclonal anti-α-tubulin (clone DM 1A; Sigma), 1:20,000. Horseradish peroxidase-conjugated anti-rabbit (1:5,000) and anti-mouse (1:2,500) secondary antibodies (GE Healthcare) and the ECL enhanced chemiluminescence reagent (PerkinElmer) were used to detect primary antibodies.

Immunohistochemistry. Immunostaining of ovaries from 20-day-old females was performed as previously described (22). The dilutions for ovary stainings were as follows: anti-Mxt 2104 (affinity purified), 1:1,000; anti-Mxt 2103, 1:1,000 (serum) or 1:250 (affinity purified); rabbit affinity-purified anti-eIF4E-1 36530 (15), 1:1,000; mouse anti-ADD87-Hts (monoclonal antibody 1B1; Developmental Studies Hybridoma Bank), 1:25; rabbit or rat anti-Mei-P26 (22, 23), 1:500; mouse anti-Orb (Developmental Studies Hybridoma Bank), 1:50; rabbit anti-eIF3j (a kind gift from M. Hentze, EMBL, Heidelberg, Germany), 1:200; and mouse anti-GFP (monoclonal antibody 3E6; Molecular Probes), 1:200. Fluorescent Alexa Fluor 488- or 546-conjugated secondary antibodies (Molecular Probes) were used at a dilution of 1:500 to detect primary antibodies on a confocal microscope (LSM510; Carl Zeiss, Inc.).

Fluorescent RNA *in situ* hybridization experiments on *Drosophila* embryos were performed using a digoxigenin (DIG)-UTP-labeled (Roche) *fushi tarazu* (*ftz*) antisense RNA probe. The *in situ* hybridization and the detection of the signal using fluorescent antibodies were performed as previously described (24).

Far-Western blotting. Far-Western analysis was performed as described previously (12). Recombinant FLAG-HMK-4E-1 was radiolabeled (^{32}P) with bovine heart muscle kinase (Sigma) and used as a probe at a concentration of 250,000 cpm/ml.

Yeast two-hybrid system. Interactions between bait and prey proteins were detected by following a yeast (*Saccharomyces cerevisiae*) interaction mating method using the strains PJ69-4A and PJ69-4a (14). Diploid cells containing both bait and prey plasmids were grown in selective medium (−Trp, −Leu) and used as a growth control. Protein interactions were detected by replica plating diploid cells onto selective media (−Trp, −Leu, −Ade, or −Trp, −Leu, −His plus 30 mM 3-amino-1,2,4-triazole [3AT]). Growth was scored after 4 days of growth at 30°C.

Cell culture and transfection. *Drosophila* Schneider 2 (S2) cells were grown in Schneider's medium containing L-glutamine (Gibco-BRL) supplemented with 10% heat-inactivated fetal bovine serum (Gibco-BRL) and penicillin-streptomycin-glutamine (100 U/ml, 100 μg/ml, and 0.292 mg/ml, respectively; Gibco BRL). Cells were grown at 25°C in 75-cm^2 flasks to 70% confluence and split every 4 days. Cells were transfected with the indicated plasmids using the Effectene transfection kit (Qiagen) according to the manufacturer's instructions. For coimmunoprecipitation (co-IP) experiments, 3×10^6 cells were transferred to a 25-cm^2 flask (~70% confluence) and transfected with 6 μg of each indicated plasmid. The cells were harvested after 24 h. For pMT plasmids, 12 h after transfection, expression was induced with 500 μM $CuSO_4$ for 24 h and then cells were harvested. Cells were washed once in 1 ml cold phosphate-buffered saline (PBS) and processed immediately afterward.

Co-IP from ovaries and S2 cells. For co-IP experiments, ovaries were dissected from 3- to 5-day-old females in cold PBS. For each IP, PBS was removed and 80 ovary pairs were ground on ice in 250 μl IP buffer (50 mM Tris-HCl [pH 8.0], 150 mM NaCl, 2 mM $MgCl_2$, 1% NP-40, and complete EDTA-free protease inhibitor cocktail). For co-IPs from S2 cells, transfected cells from one 25-cm^2 flask were lysed on ice in 1 ml IP buffer. Lysates were spun for 10 min at 13,000 rpm at 4°C, and the supernatant was precleared for 1 h at 4°C with 50 μl (for ovaries) or 200 μl (for S2 cells) of a 50% slurry of protein G-Sepharose beads (4 Fast Flow; GE Healthcare) equilibrated in IP buffer. A total of 450 μl (for S2 cells) of the supernatant was then transferred to another tube containing 30 μl of the 50% slurry of protein G-Sepharose beads equilibrated in IP buffer, supplemented either with RNAsin (Promega) or RNase A (0.35 mg/ml) and either primary antibody (5 μl for anti-HA, 1.5 μl for anti-Mxt, 3 μl for anti-V5; or 1.5 μl of anti-eIF4E), 1.5 μl of the corresponding preimmune serum, or nothing. For mouse monoclonal anti-HA antibodies (Sc 7392; Santa Cruz), 5 μl (0.2 μg/μl) per IP was used. The mixture was rotated for 3 h (5 h in the case of eIF3b IP) at 4°C, and the beads were then washed 5 times with 1.5 ml IP buffer, standing for 15 min on ice between washes. Afterwards, Laemmli sample buffer was added to the beads, which were boiled for 5 min and analyzed by SDS-PAGE and immunoblotting.

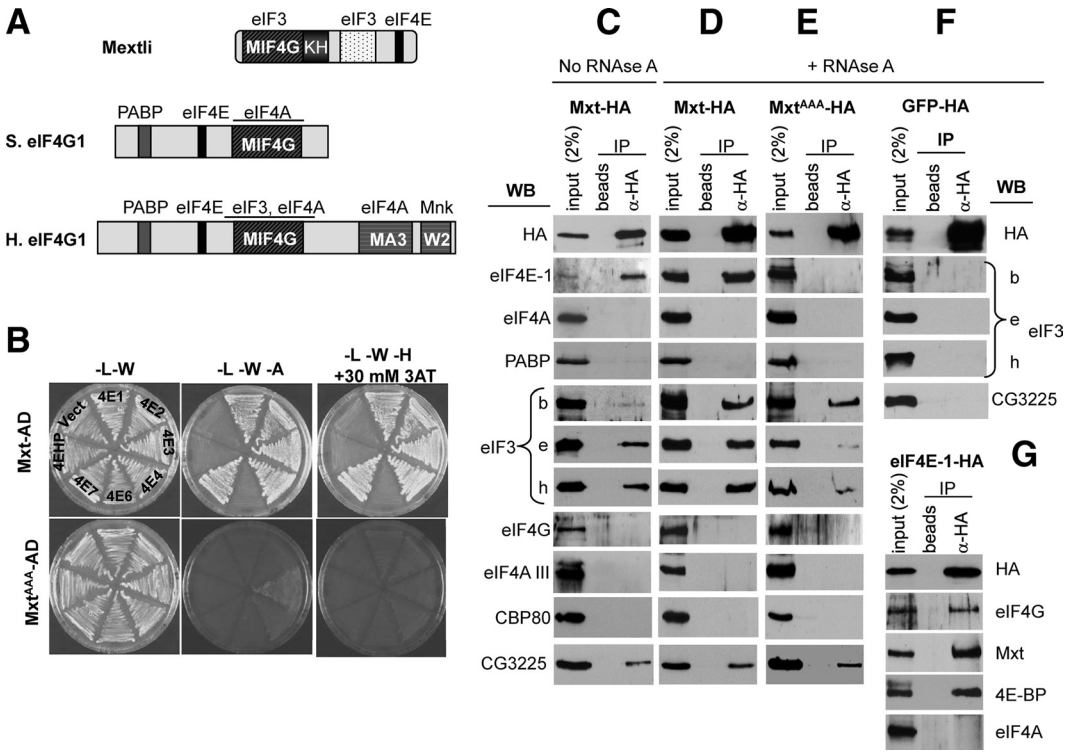

FIG 1 Mxt is a novel type of eIF4E-interacting protein that binds RNA, eIF4Es, eIF3, and CG3225. (A) Schematic representation of the domain structure and interactions of Mextli, *Saccharomyces cerevisiae* (S.) eIF4G1, and human (H.) eIF4G. The MIF4G (amino acids 1 to 130), KH RNA binding domains (amino acids 240 to 279), and the eIF4E-binding motif (amino acids 581 to 587) of Mxt are indicated. (B) Mxt interacts with eIF4E-1, -2, -3, -4, and -7 in the yeast two-hybrid system via the eIF4E-binding site. -L, −Leu; -W, −Trp; -A, −Ade; -H, −His. (C to G) Coimmunoprecipitation experiments showing that Mxt physically interacts with eIF4E-1, eIF3, and the helicase encoded by the annotated gene CG3225. eIF3e, eIF3h, and CG3225 are in fusion with the V5 epitope. Plasmids expressing 3×HA-tagged versions of Mxt (C and D), Mxt^{AAA} (E), GFP (negative control) (F), or eIF4E-1 (G) were transfected into S2 cells. For a schematic representation of the constructs used (3×HA-Mxt and 3×HA-Mxt^{AAA}), see Fig. 2A. (G) HA-eIF4E-1 physically interacts with endogenous Mxt, eIF4G, and 4E-BP (Thor). Immunoprecipitations (IP) were conducted using either beads alone or beads plus anti-HA antibodies in the absence (C) or presence (D, E, F, and G) of RNase A, and interactions were detected by immunoblotting.

Translation assays. *In vitro* translation assays using ovary cell-free lysates was performed as described previously (25). Luciferase activities were measured in a 20/20 luminometer (Turner BioSystems).

Cap affinity chromatography. Fifty micrograms of total protein in 500 μl cap-binding buffer (CBB) (100 mM KCl, 20 mM HEPES-KOH [pH 7.6], 7 mM β-mercaptoethanol, 0.2 mM EDTA, 10% glycerol, 0.1% Triton X-100, 50 mM β-glycerol phosphate, 50 mM NaF, 100 μM sodium orthovanadate, 0.1 mM GTP, complete EDTA-free protease inhibitor cocktail) was precleared with 200 μl Sepharose 4B CL for 1 h at 4°C and then incubated for 1 h with 50 μl of m^{7}GTP-Sepharose 4B (GE Healthcare) at 4°C. The supernatant was recovered (unbound fraction), and the resin was washed three times with 1,500 μl of CBB and resuspended in Laemmli sample buffer (bound fraction). Proteins from the unbound fractions were precipitated with 20% trichloroacetic acid (TCA) and resuspended in sample buffer. Proteins were subjected to SDS-PAGE and further Western blot analyses.

***Drosophila* strains and fly work.** Oregon-R or *yw* (yellow-white) flies served as wild-type controls, as indicated. The *yw*; *P*{$^{w+}$, UAS-*Mxt-V5*} and *yw*; *P*{*w*$^+$, UAS-*Mxt*^{AAA}*-V5*} transgenic flies were generated by microinjection of the constructs pUASP-Mxt-V5 or pUASP-Mxt^{AAA}-V5 into embryos of the *yw*; *J*; *15 attP-86F* (*3R*) strain (13) for directed insertion into chromosome *3R*. The *GFP-eIF4E1* (stock *YC0001*) protein trap strain was obtained from the GFP protein trap line collection (26). Flies of the *w*^{1118}; *Df(2L)Exel6010*, *P*{*w*$^{+mC}$=*XP-U*}*Exel6010*/*CyO* (27), *ts14*/*CyO*;*ry*^{506} *e*^{1} *bam*$^{\Delta 86}$/*TM3*, *ry*^{RK} *Sb*^{1} *Ser*^{1} (28), and *mei-P26*^{fs1} (22) strains and the maternal driver tub-Gal4 *w**; *P*{*w*$^{+mC}$=*matα4-GAL-VP16*}*V37* strain were obtained from the Bloomington *Drosophila* Stock Center. *yw*; *PBac*{*RB*}*CG2950*^{e00436}/*CyO* and *yw*; *PBac*{*WH*}*CG2950*^{f01505}/*CyO* (29) flies were obtained from the Exelixis Collection at Harvard.

Hatching tests were performed at 25°C. Animals were mated for 2 days, and then eggs were collected for 9 h on juice-agar plates. Eggs randomly chosen were transferred to another plate, and unhatched eggs were scored after 40 h of further incubation at 25°C. Cuticles were then prepared from the unhatched eggs from transheterozygous *mxt*^{e00436}/*Df(2L)Exel6010* females according to reference 30.

Egg-laying tests were performed at 25°C. Females of the indicated phenotype were mated with Oregon-R males in regular food bottles. For each phenotype, every 5 days three cages with agar-apple juice were set with 20 females and 20 males each for 24 h. Flies were removed, and the eggs were counted.

Northern blotting. To perform Northern blot analysis, 7.5 μg of poly(A)$^+$ extracted from adults was blotted and probed with an *mxt* cDNA probe according to reference 31.

Crude extract preparation. Total lysates of wild-type (Oregon-R) *Drosophila* staged animals were prepared by disruption on ice of 1 g tissue per ml buffer containing 8 M urea, 20 mM HEPES-KOH (pH 7.5), 100 mM KCl, 2 mM EDTA, 0.5% Triton X-100, 1 mM dithiothreitol (DTT), 2 mM PMSF, and complete EDTA-free protease inhibitor cocktail (Roche, GmbH), followed by centrifugation at 14,000 rpm for 10 min at 4°C. The supernatant was recovered and stored at −80°C. The protein concentration of the samples was quantified with the Bio-Rad protein assay kit.

Poly(A)-Sepharose pulldown. A total of 6 × 10^6 S2 cells were transferred to a 25-cm^2 flask (~70% confluence) and either transfected with 6 μg of plasmid pMT-Mxt or pAWH-Mxt or not transfected at all. Thirty-

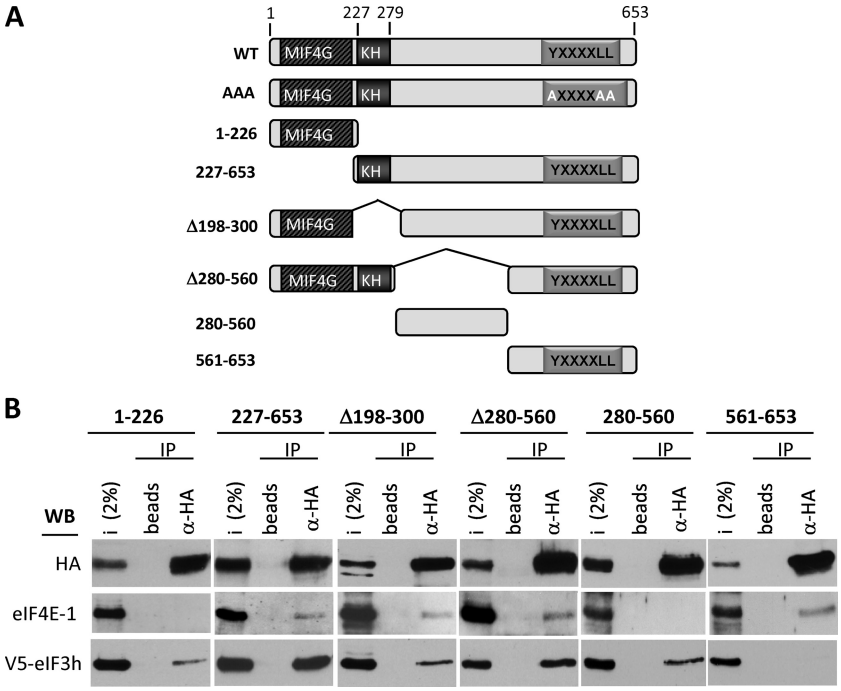

FIG 2 Mapping of Mxt regions for interaction with eIF4E-1 and eIF3. (A) Plasmids that express different 3×HA-tagged regions of Mxt in S2 cells. The 3×HA-Mxt and 3×HA-Mxt^{AAA} constructs were used in Fig. 1C to E. (B) The plasmids depicted in panel A were either transfected into S2 cells alone or cotransfected with a plasmid expressing a V5-tagged version of eIF3h. Total extracts of transfected cells were used to perform immunoprecipitation experiments using either beads alone or beads plus anti-HA antibodies in the presence of RNase A. Samples were then subjected to Western blotting (WB) using either anti-eIF4E-1 or anti-V5 antibodies. i, input.

six hours later, cells were harvested. In the case of pMT-Mxt, 12 h after transfection, cells were induced with 500 μM $CuSO_4$ for 24 h and then harvested. Cells were harvested, washed in 1 ml cold PBS, and lysed on ice in 500 μl buffer A (150 mM NaCl, 50 mM Tris-HCl [pH 7.4], 1% NP-40, 1 mM DTT, 2 mM $MgCl_2$, RNasin, complete EDTA-free protease inhibitor cocktail). Lysates were spun 10 min at 13,000 rpm at 4°C. A total of 250 μl of the supernatant was incubated with 50 μl of either Sepharose 4B CL or poly(A)-Sepharose 4B CL (Amersham Pharmacia Biotech, AB). The mixture was rotated for 3 h at 4°C, and then the beads were washed five times with 1.5 ml buffer A on ice with 20 min between washes. Afterwards, Laemmli sample buffer was added to the beads, and the mixture was boiled for 5 min and analyzed by SDS-PAGE and further Western blotting with the indicated antibodies.

RESULTS

Mextli is a novel type of eIF4E-binding protein. Despite the existence of several cognates of eIF4E in *Drosophila* (8, 32), eIF4E-1 is essential throughout embryogenesis, and global cap-dependent translation relies mainly on this isoform (8, 15). We sought to identify new proteins that interact with eIF4E-1 and are involved in specific developmental events. To this end, a 20- to 22-h embryonic *Drosophila* cDNA expression library was screened by far-Western blotting using ^{32}P-labeled FLAG-HMK-eIF4E-1 as a probe. Five positive cDNAs were recovered—one encoding 4E-BP (*Thor*) (20) and four corresponding to the annotated gene CG2950, which encodes a 653-amino-acid protein with a molecular mass of 70.149 kDa. We termed this novel 4E-BP "Mextli" (Mxt), after the Aztec god of storms and war. To gain insight into the function of Mxt, we searched protein databases for similarities in the primary sequence (11), predicted secondary structural regions of α-helices, loops, and β-strands, and solvent accessibility (9, 10). The Mxt amino-terminal region (amino acids 1 to 130) contains an MIF4G domain (33, 34) (Fig. 1A). Mxt harbors in the middle region (amino acids 240 to 279) an RNA-binding KH domain of the "mini-KH" class (35) containing the hallmark G-X-X-G motif at amino acids 244 to 247. Mxt also possesses a canonical eIF4E-binding motif, YXXXXLL (amino acids 581 to 587), at its carboxy-terminal end (Fig. 1A). This unique, modular structure has not previously been found in any 4E-BP, rendering Mxt a novel type of 4E-BP. A comparison of Mxt structure with those of the yeast and human eIF4Gs shows that Mxt resembles eIF4G, but the sequential order of the domains in Mxt differs from that in eIF4G with respect to their N- to C-terminal arrangement (Fig. 1A). Mxt orthologues exist in all Drosophilidae species and in other metazoans, such as in the Coleoptera and Culicinae, as well as in *Caenorhabditis elegans* (protein Y18D10A.8), but not in vertebrates.

Mxt is a scaffold protein for translation initiation factors. To determine whether the putative eIF4E-binding site of Mxt is required for the interaction with eIF4E-1 and whether Mxt binds other *Drosophila* eIF4E cognates, a yeast two-hybrid assay was performed using eIF4Es as "bait" plasmids and Mxt constructs as "prey" (Fig. 1B). Clear interactions were detected between Mxt and eIF4E-1, eIF4E-2, eIF4E-3, eIF4E-4, and eIF4E-7 but not with eIF4E-6 and 4E-HP. The lack of interaction of Mxt with eIF4E-6 and 4E-HP was confirmed by coimmunoprecipitation experiments (see Fig. S1 in the supplemental material). Mutations of three residues within the consensus eIF4E-binding motif of Mxt (Tyr581, Leu586, and Leu587) to Ala (here named "Mxt^{AAA}") abolished the interaction of eIF4Es with Mxt (Fig. 1B). These in-

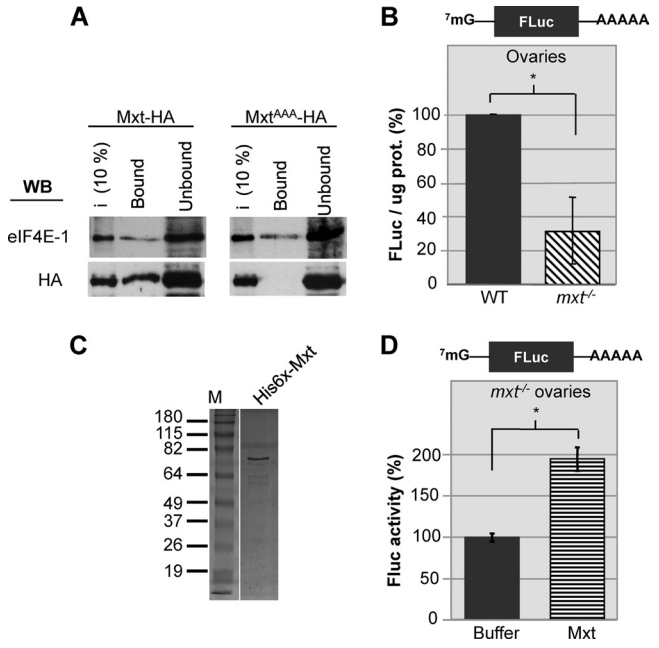

FIG 3 Mxt promotes translation. (A) m^{7}GTP-Sepharose pulldown. Plasmids expressing 3×HA-tagged versions of Mxt or Mxt^{AAA} were transfected into S2 cells, and 50 μg of total extract of transfected cells was subjected to m^{7}GTP-Sepharose chromatography. Bound and unbound fractions were then subjected to SDS-PAGE and Western blotting using anti-HA or anti-eIF4E-1 antibodies. i, input. (B) Luciferase assays measuring translation of an m^{7}G-capped and polyadenylated firefly luciferase reporter (FLuc) mRNA in cell-free ovary lysates from *yw* (wild-type) or homozygous *mxt*^{e00436} (*mxt*$^{-/-}$) females. The bars represent the results of five independent experiments ($P < 0.001$). (C) Coomassie blue staining of recombinant 6×His-Mxt protein. Lane M, molecular mass markers (kDa). (D) Luciferase assays measuring translation in homozygous *mxt*^{e00436} (*mxt*$^{-/-}$) ovary lysates supplemented with either buffer or 0.2 μg of recombinant 6×His-Mxt. *, $P < 0.001$.

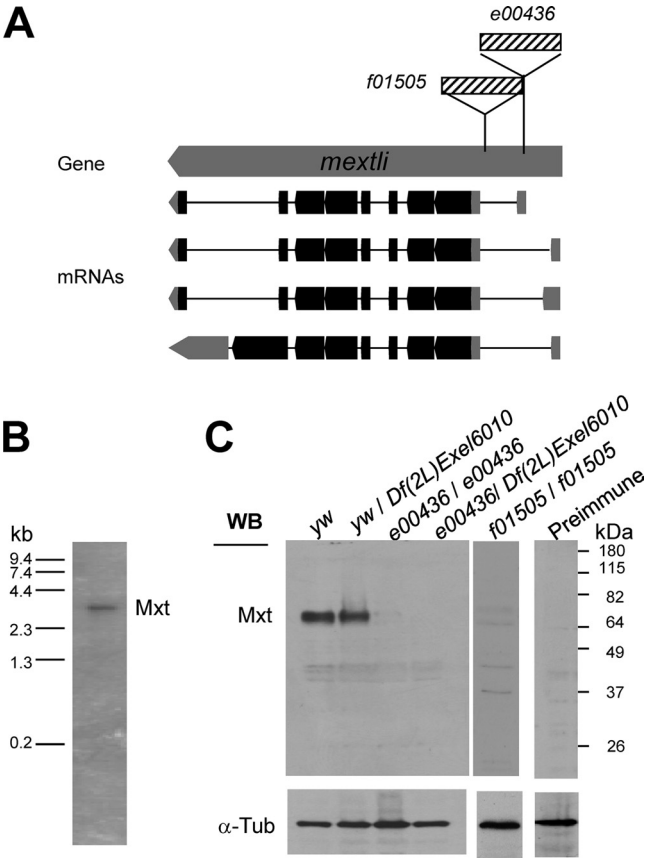

FIG 4 Structure and expression of the *mxt* gene. (A) Schematic diagram of the *mxt* gene (CG2950) showing predicted transcripts and sites of the PiggyBac insertions *f01505* and *e00436*. (B) Northern analysis shows that *mxt* mRNA is ~3.7 kb in length. (C) Western blot analysis shows that affinity-purified anti-Mxt antibodies (2101) recognize a single polypeptide band of the predicted molecular mass of Mxt (70 kDa) in total extracts (15 μg per lane) that is greatly reduced in *mxt* mutants. Similar results were obtained with affinity-purified anti-Mxt antibodies 2103 and 2104 (data not shown). α-Tub, α-tubulin.

teractions were insensitive to RNase, indicating that the interactions are direct. The interaction between Mxt and eIF4E-1 via the consensus eIF4E-binding motif of Mxt was further corroborated by both far-Western blotting (see Fig. S2 in the supplemental material) and coimmunoprecipitation experiments (Fig. 1E, 2B, 3A; see Fig. 8C to E).

To determine whether other translation initiation factors copurify with Mxt, S2 cells were transfected with HA-tagged Mxt and immunoprecipitation experiments were performed using an anti-HA antibody. Interestingly, eIF3 and the DEAH-box DNA/RNA helicase encoded by CG3225 coimmunoprecipitated with Mxt, but eIF4G, eIF4A, eIF4AIII, and CBP80 did not (Fig. 1C). These additional associations were insensitive to RNase treatment (Fig. 1D) and were unaffected by mutation of the eIF4E-binding domain (Fig. 1E), indicating that they are direct interactions. In parallel control experiments, none of these proteins interacted with GFP (Fig. 1F). To further corroborate these results, S2 cells were transfected with an HA-tagged version of eIF4E-1 and coimmunoprecipitations were performed to compare the ability of HA–eIF4E-1 to interact with endogenous Mxt and other known eIF4E-interacting proteins, namely, eIF4G and 4E-BP (Fig. 1G). Mxt exhibited the strongest affinity for eIF4E-1. As expected, eIF4E-1 did not interact with eIF4A (negative control).

To map the regions of Mxt required for its interaction with eIF3, several HA-tagged deletion constructs were expressed in S2 cells (Fig. 2A) and examined for their ability to interact with eIF4E and eIF3. In coimmunoprecipitation experiments, two truncated forms of Mxt, one including amino acids 227 to 653 and one with amino acids 280 to 560 deleted, showed the strongest associations with eIF3 (Fig. 2B). These two forms share only amino acids 227 to 279, which include the KH domain, and the C-terminal end (amino acids 561 to 653). The C-terminal fragment of Mxt alone (amino acids 561 to 653) shows very little interaction with eIF3 in similar experiments (Fig. 2B). Three truncated forms of Mxt that lack the KH domain-containing region (aa 1 to 226, Δ198–300, and aa 280 to 560) associate with eIF3, but less strongly than the two forms containing the KH domain, as deduced from comparing the ratio of bound material (anti-HA) to input (i) in each experiment. These results do not allow us to implicate a specific segment of Mxt as essential for eIF3 binding, although they do suggest that a region that includes the KH domain contributes substantially to this interaction. As expected, eIF4E-1 interacted with all Mxt fragments containing the motif YXXXXLL but not with those fragments lacking it (Fig. 2B). Taken together, our results show that Mxt can bind to several eIF4E isoforms (eIF4E-1, -2, -3, -4, and -7), the helicase CG3225, and eIF3. These results are

A

Hatching test of *mxt* mutants

	Females			Males		
Genotype	***+/Df***	***436/Df***	***505/Df***	***+/Df***	***436/Df***	***505/Df***
n=	1893	667	596	431	323	792
Hatched eggs	97%	78.7%	86.6%	93.7%	96%	92.7%
P value		<0.0001	<0.0001		0.175	0.488

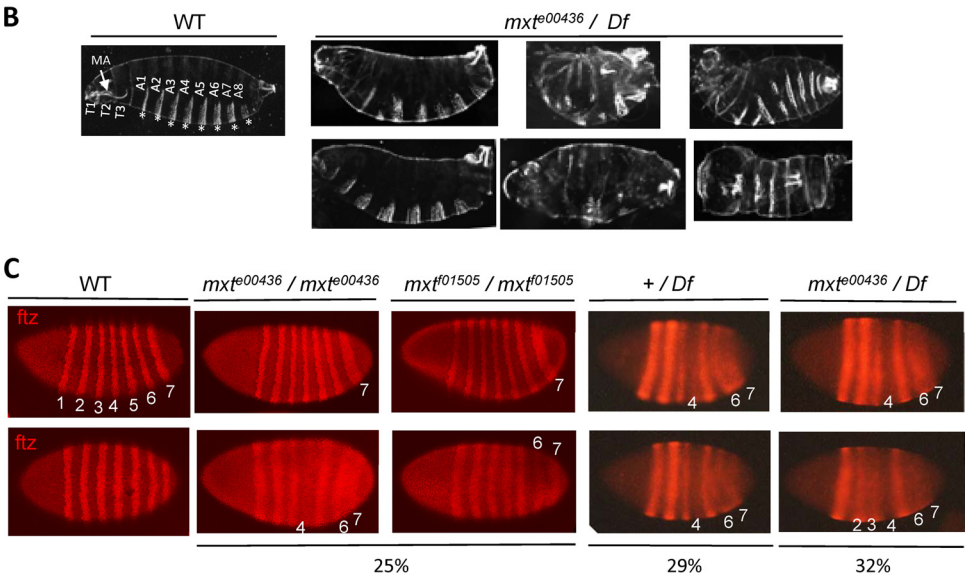

FIG 5 Maternal loss of *mxt* function affects embryogenesis. (A) Hatching test. Females or males of the indicated phenotype were mated with wild-type (WT) (Oregon-R) animals of the opposite sex, and eggs that failed to hatch were counted. Hatching rates were significantly lower among embryos produced by *mxt* females than among those from wild-type females. (B) Cuticle preparations from wild-type embryos and embryos that were produced by mxt^{e00436}/*Df*(*2L*)*Exel6010* females and failed to hatch. Thoracic (T1 to T3) and abdominal (A1 to A8) segments, mouth apparatus (MA), and the denticle belts (*) are labeled in the wild-type embryo. Embryos from *mxt* females exhibit various segmentation defects, including deletion of one or more thoracic or abdominal segments (left panels), severe global defects (middle panels), or malformation or incomplete development of abdominal segments (right panels). (C) *In situ* hybridization experiments for *ftz* mRNA in embryos produced by females of the indicated genotypes. The seven *ftz* stripes in the wild-type embryo are labeled and numbered. *mxt* mutants showed partial or total deletion of the fourth stripe and/or fusion of sixth and seventh stripes or widening of the seventh stripe. These defects were found in 25 to 32% of embryos produced by mutant females, as indicated.

consistent with previous observations from high-throughput interaction screens reporting direct interactions of Mxt and its *Caenorhabditis elegans* homolog with several eIF4E isoforms (36, 37) and with eIF3 (38).

Mxt promotes translation. To determine the functional importance of Mxt binding to eIF4E, we investigated whether Mxt can interact with endogenous eIF4E when the latter is bound to the cap structure. S2 cells were transfected either with Mxt-HA or Mxt^{AAA}-HA, and pulldown assays were performed using an m^7GTP-Sepharose resin (Fig. 3A). Wild-type Mxt-HA was retained on the resin, but Mxt^{AAA}-HA was not, demonstrating that the association of Mxt with the 5′-cap structure requires it to bind eIF4E.

To investigate the role of Mxt in translation, *in vitro* translation assays were performed using cell-free ovary extracts prepared from either wild-type or *mxt* mutant flies (see below) with a cap-dependent luciferase reporter mRNA. Cap-dependent translation in *mxt* mutant extracts was reduced by 3-fold in comparison to that in the wild type (Fig. 3B). This effect was largely rescued by addition of recombinant His_6-Mxt (Fig. 3C) to the mutant extracts (Fig. 3D).

***mxt* functions in early oogenesis and embryogenesis.** *mxt* is a single-copy gene with three predicted transcripts that differ only in the 5′ UTR (Fig. 4A). These mRNAs encode the same 653-amino-acid polypeptide. There is a fourth annotated putative transcript that is substantially longer than the other three mRNAs, which would encode a larger protein. On Northern and Western blots, we observed only a single mRNA species consistent with the size of the smaller mRNAs and a single protein migrating at ~70 kDa (Fig. 4B and C). Two homozygous viable PiggyBac insertions, *PBac*{*RB*}*CG2950*^{e00436} and *PBac*{*WH*}*CG2950*^{f01505} (29), whose insertion sites were confirmed by PCR experiments using total genomic DNA from homozygous flies (data not shown), interrupt the 5′ UTR of *mxt* (Fig. 4A). These insertions led to a severe reduction in Mxt protein levels, as determined by using specific antibodies against Mxt in Western blot analyses (Fig. 4C).

Strains carrying both *mxt* alleles, either when homozygous or in *trans* with the chromosome deficiency mutation

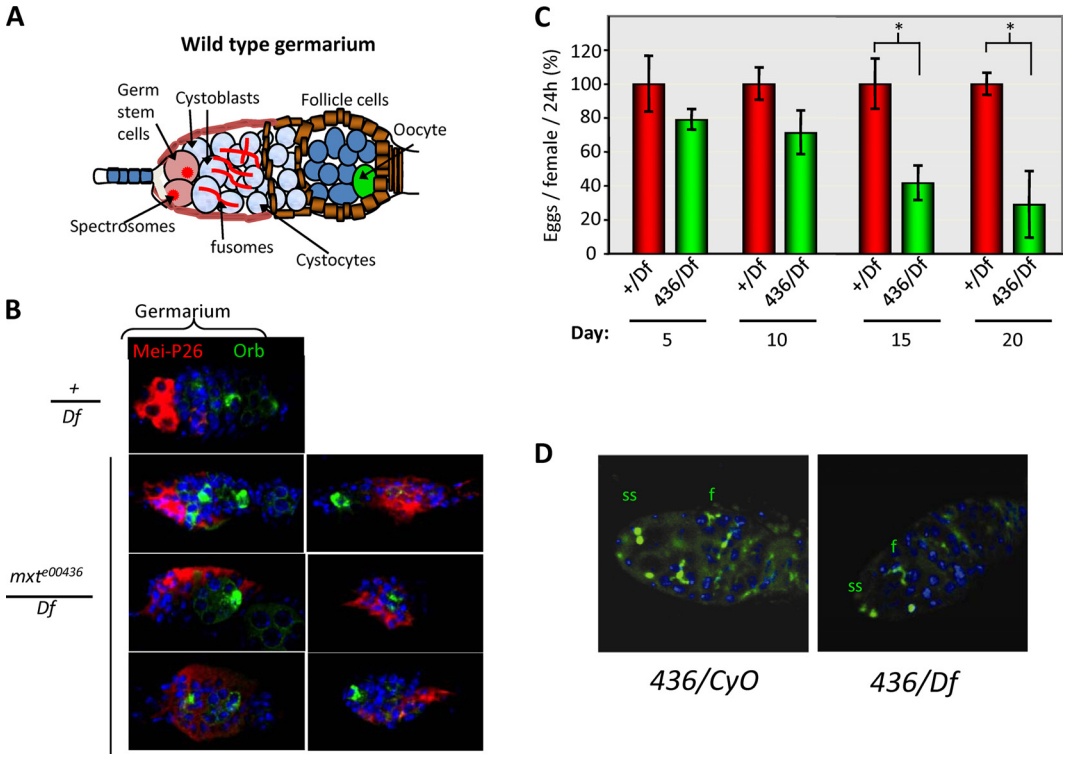

FIG 6 *mxt* mutations affect germarium morphology and female fertility. (A) Schematic diagram of the *Drosophila* germarium. Germ line stem cells (GSCs) divide asymmetrically to form another GSC and a cystoblast, which will subsequently divide to give rise to 16 germ line cells, one of which will differentiate into the oocyte. The remainder will become nurse cells. Each GSC and cystoblast contains a spectrosome. During transit-amplifying divisions, the spectrosome develops into a branched structure called the fusome, which extends through cytoplasmic bridges through each germ line cell and orients the axes of the cell divisions (62). (B) Immunostaining of ovaries from 20-day-old females of the indicated genotypes with Mei-P26 (red), Orb (green), and the nuclear stain DAPI (4′,6-diamidino-2-phenylindole) (blue). (C) Egg-laying tests of $mxt^{e00436}/Df(2L)Exel6010$ (green bars) and $+/Df(2L)Exel6010$ (red bars; control) females. $mxt^{e00436}/Df(2L)Exel6010$ females produce significantly fewer eggs ($P < 0.005$ after 15 days of aging) over time than control females. (D) Immunostaining of germaria from 21-day-old mxt^{e00436}/CyO (*436/CyO*) and $mxt^{e00436}/Df(2L)Exel6010$ (*436/Df*) ovaries with anti-Add87/Hts (1B1) antibodies. Spectrosomes (ss) and branched fusomes (f) are labeled. $mxt^{e00436}/Df(2L)Exel6010$ germaria contained fewer spectrosomes, which are present in germ line stem cells and cystoblasts, than the heterozygous control.

Df(2L)Exel6010 (27), which includes *mxt*, are viable and fertile. However, a substantial proportion (14 to 21%, depending on the *mxt* allele) of embryos produced by *mxt/Df(2L)Exel6010* females failed to hatch (Fig. 5A). Cuticle preparations made from embryos produced by $mxt^{e00436}/Df(2L)Exel6010$ females that failed to hatch (~21%) showed variable segmentation defects affecting anterior-posterior patterning (Fig. 5B). Consistent with this, *in situ* hybridization to *fushi tarazu* (*ftz*) mRNA on early embryos produced by *mxt* homozygous females indicated that a similar proportion had deletion of the fourth stripe as well as fusion or broadening of the sixth and seventh stripes (Fig. 5C). This proportion increased to 32% in embryos produced by $mxt^{e00436}/Df(2L)Exel6010$ females. These results confirm that maternal loss of Mxt affects early embryogenesis.

Next, the morphology of *mxt* ovaries was analyzed. We noticed that *mxt/Df(2L)Exel6010* ovaries are generally smaller than those of heterozygous controls or the wild type, and fewer late-stage oocytes are present. To examine this more closely, we used anti-Mei-P26 antibodies, which mark germ line stem cells (GSCs) and dividing cystocytes, and anti-Orb antibodies, which mark the oocyte, to stain ovaries. These experiments revealed developmental defects in $mxt^{e00436}/Df(2L)Exel6010$ germaria (Fig. 6B). In wild-type ovaries, Mei-P26-positive GSCs and dividing cystocytes are located at the anterior of the germarium, and 16-cell cysts that have differentiated oocytes, which are positive for Orb, are located more posteriorly. In contrast, in many $mxt^{e00436}/Df(2L)Exel6010$ germaria, Mei-P26 expression extends abnormally toward the posterior, with Mei-P26-positive cells partially or completely surrounding cysts that contain an Orb-positive cell (Fig. 6B). Next, we compared the fecundity of $mxt^{e00436}/Df(2L)Exel6010$ and $+/Df(2L)Exel6010$ (control) females. We observed that young (5-day-old) $mxt^{e00436}/Df(2L)Exel6010$ females produced ~80% as many eggs as controls, but the difference between $mxt^{e00436}/Df(2L)Exel6010$ females and controls was much more pronounced when older animals were compared (egg laying of ~25% of that of the control after 20 days) (Fig. 6C). Consistently, we found fewer germ line cells in the germaria of aged (21-day-old) $mxt^{e00436}/Df(2L)Exel6010$ females than in wild-type controls. Using a monoclonal antibody directed against anti-ADD87-Hts (1B1) staining that marks spectrosomes and fusomes, we counted spectrosomes, structures that are present in GSCs and cystocytes but not in germ line cells in cysts containing two or more cells (Fig. 6D). $mxt^{e00436}/Df(2L)Exel6010$ ovaries had 4.85 ± 1.41 spectrosome-positive cells, compared with 6.33 ± 1.63 in mxt^{e00436}/CyO controls. These results support the notion that *mxt* plays a role in GSC maintenance.

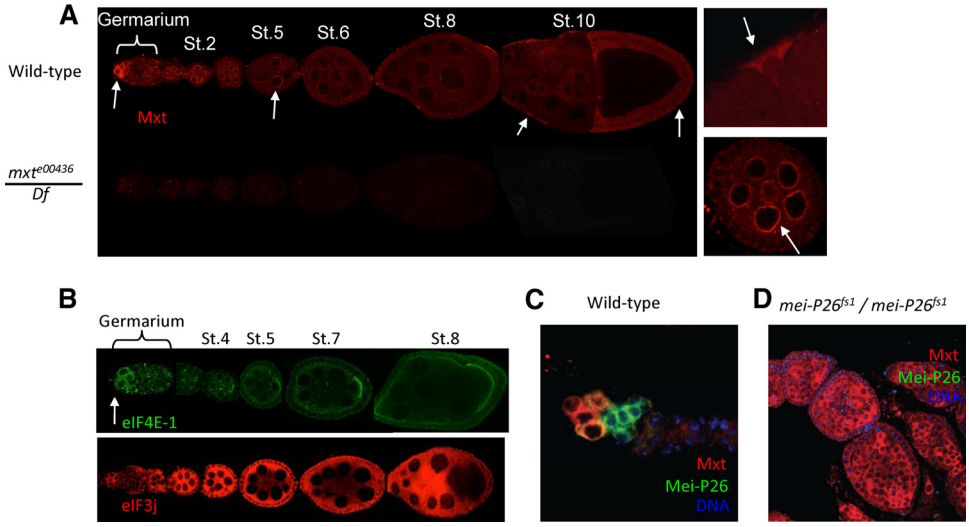

FIG 7 Mextli and eIF4Es expression during oogenesis. (A) Composites of multiple images depicting immunostaining of wild-type (Oregon-R) or *mxt*^{e00436}/*Df*(*2L*)*Exel6010* ovarioles (negative control) with anti-Mxt antibodies. Mxt is cytoplasmic and enriched in the GSCs and cystoblasts and in the perinuclear nuage. Somatic expression in stretched cells and columnar follicular cells is also apparent. Arrows indicate sites of high Mxt concentration. The right panels show magnified stage (St.) 10 (upper panel) and stage 4 (lower panel) egg chambers with enrichment of Mxt (arrows) in the cytoplasm of a stretched cell and in the perinuclear region of nurse cells, respectively. (B) Composites of multiple images depicting immunostaining of wild-type ovaries with anti-eIF4E-1 or anti-eIF3j antisera. Note the enrichment of eIF4E-1 in the GSCs and cystoblasts (white arrow). (C) Immunostaining of wild-type germaria with anti-Mxt and anti-Mei-P26 antisera. Mxt expression is high in GSCs and cystocytes but reduced in transit-amplifying cells, where Mei-P26 expression peaks. (D) Immunostaining of *mei-P26*^{fs1}/*mei-P26*^{mfs1} ovaries with anti-Mxt and anti-Mei-P26 antisera. Mxt expression levels are heterogeneous among undifferentiated germ cells within individual tumorous egg chambers.

We then analyzed the expression of Mxt during oogenesis. Immunostaining revealed that while Mxt is expressed throughout oogenesis, its level is particularly high in GSCs and cystoblasts (Fig. 7A). The Mxt level diminishes through subsequent transit-amplifying divisions (Fig. 7A). In germ line cells, Mxt is predominantly cytoplasmic, and it gradually accumulates in the perinuclear nuage, beginning at stages 2 to 3. This expression pattern is consistent with the developmental defects we observed in *mxt* ovaries and with a role of Mxt in GSC maintenance. Around stage 8, Mxt disappears from the perinuclear nuage, but it remains detectable in the nurse cells and oocyte cytoplasm. At about the same developmental stage, Mxt expression is increased in follicle cells, where it persists into late oogenesis, both in stretched cells and in columnar follicle cells (arrows in Fig. 7A). Mxt is also expressed in somatic cells during other developmental stages (see Fig. S3 in the supplemental material).

The high expression of Mxt in GSCs and cystoblasts is very intriguing, as the eIF4E-1 level must be tightly regulated in GSCs to prevent them from becoming cancer stem cell-like cells (39). Moreover, an abundance of eIF4E-1 in GSCs was observed using the *GFP-eIF4E-1* trap line (26, 40) and in immunostaining experiments (39). Consistent with these results, using Western blotting (41) and immunostaining experiments (Fig. 7B), we found that eIF4E-1 is expressed in ovaries and that eIF4E-1 is highly expressed in GSCs and early-stage cystocytes in a very similar pattern as Mxt (Fig. 7B). As well, we observed that eIF3 (visualized by immunostaining for the eIF3j subunit) is also enriched in the tip of the germarium in GSCs and cystocytes (Fig. 7B). These coincident expression patterns suggest that Mxt, eIF4E-1, and eIF3 could interact in GSCs and early-stage cystocytes. We also examined Mxt expression in *mei-P26*^{fs1}/*mei-P26*^{mfs1} ovaries, where germ cell differentiation is abrogated and the germ line consists of tumors of undifferentiated cells that express high levels of eIF4E-1 (39). We found that Mxt expression was heterogeneous within these tumors (Fig. 7C and D), with some cells expressing levels comparable to those of GSCs and others expressing levels lower than those of transit-amplifying cells. In *mei-P26* mutants, Mxt is expressed at high levels throughout the germarium, suggesting that downregulation of Mxt is important for nurse cell and oocyte specification.

To further investigate the distribution and interaction of Mxt and eIF4E-1 in GSCs and early cystocytes, we performed coimmunostaining of wild-type germaria using 1B1 antibodies along with either anti-Mxt or anti-eIF4E-1 antibodies, as well as Mxt immunostaining of germaria from the *GFP-eIF4E-1* line. Both Mxt and eIF4E-1 were enriched and colocalized in cells that have a single focus of 1B1 signal, namely, GSCs and cystoblasts (Fig. 8A and B). To demonstrate that Mxt and eIF4E-1 physically interact in GSCs, coimmunoprecipitation experiments were performed with extracts from null *bag-of-marbles* (*bam*) mutant germaria (*bam*^{86}), in which GSCs fail to differentiate and proliferate instead (28, 42). Anti-eIF4E-1 antibodies, but not preimmune serum, coimmunoprecipitated endogenous eIF4E-1 with Mxt from *bam*^{86} ovaries in the presence of RNase (Fig. 8C). This was also the case when extracts from wild-type ovaries were used (Fig. 8D). Importantly, anti-Mxt antibodies also coimmunoprecipitated endogenous Mxt with eIF4E-1 in the presence of RNase (Fig. 8D). No interaction was detected with preimmune sera or between these proteins and an unrelated control (α-tubulin). We also observed, using anti-Mxt antibodies, that in the presence of RNase, endogenous eIF3b and Mxt coimmunoprecipitated from wild-type ovary extracts (Fig. 8D).

To support the data demonstrating an association between eIF4E-1 and Mxt during oogenesis, we generated transgenic flies

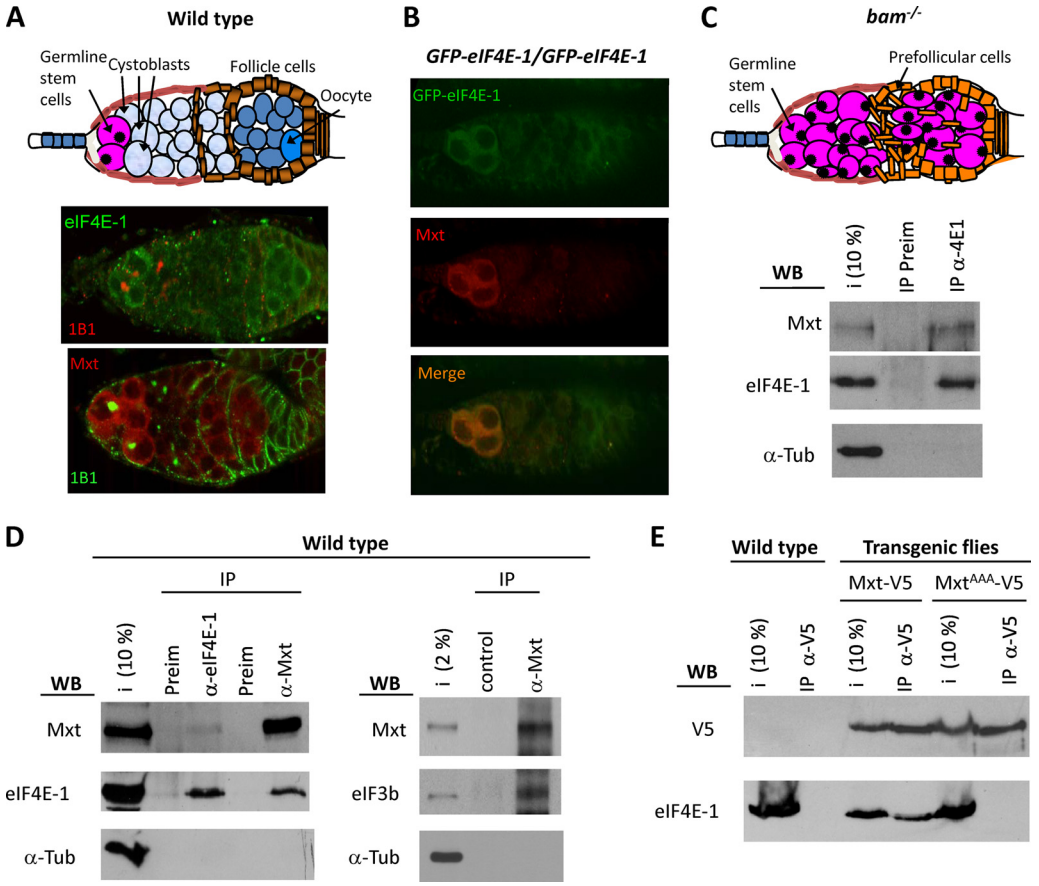

FIG 8 Mxt and eIF4E-1 colocalize and physically interact in germ line stem cells and during oogenesis. (A to C) Mxt and eIF4E-1 are enriched and colocalize in GSCs and cystoblasts. (A) Coimmunostaining of wild-type (Oregon-R) germarium with either anti-eIF4E-1 (green) and anti-ADD87-Hts (1B1; red) or anti-Mxt (red) and anti-ADD87-Hts (1B1; green). eIF4E-1 and Mxt are enriched in GSCs and cystoblasts, as marked by punctate staining with 1B1 antibody. (B) Immunostaining of germaria from *GFP-eIF4E-1/GFP-eIF4E-1* flies with anti-Mxt and anti-GFP showing results similar to those in panel A. (C) Immunoprecipitation experiments using total extracts of $bam^{-/-}$ germaria (made up mostly by GSCs) performed using either anti-eIF4E-1 antibodies or preimmune serum in the presence of RNase A showing that endogenous eIF4E-1 and Mxt can be copurified. (D) Immunoprecipitation experiments using total extracts of wild-type (Oregon-R) ovaries, again showing an association between endogenous Mxt and eIF4E-1 (left), as well as between Mxt and eIF3b (right). (E) Immunoprecipitation experiments using total extracts of ovaries either from wild-type (Oregon-R, control) or transgenic females expressing V5-tagged versions of Mxt or Mxt^{AAA}. Binding of Mxt to eIF4E-1 requires an intact consensus eIF4E-binding domain.

expressing either V5 epitope-tagged forms of wild-type Mxt or Mxt^{AAA} (which abrogates eIF4E binding) and performed coimmunoprecipitation experiments using extracts from total ovaries and anti-V5 antibodies (Fig. 8E). Endogenous eIF4E-1 coimmunoprecipitated along with Mxt-V5 protein but not with Mxt^{AAA}-V5 (Fig. 8E). Taken together, these experiments demonstrate that Mxt and eIF4E-1 are enriched in GSCs and cystoblasts and colocalize and physically interact *in vivo*, and this interaction is mediated by a canonical Mxt eIF4E-binding motif.

DISCUSSION

In this study, we provide evidence that a newly discovered eIF4E-binding protein, Mxt, forms a complex with eIF4E-1 and eIF3 that promotes translation. We also showed that loss of *mxt* leads to defects in oogenesis and to patterning defects affecting the anterior-posterior axis. Large-scale interaction screens had previously been demonstrated an association of both Mxt and its *C. elegans* homolog (protein Y18D10A.8) with several eIF4E cognates (36, 37) and Mxt with eIF3 (38) and the helicase encoded by the annotated gene CG3225 (36). Our results also agree with earlier work showing that Mxt is a component of cap-binding complexes (8) and with RNA interference (RNAi) experiments performed in *C. elegans* suggesting that Y18D10A.8 is essential for viability and fertility and important for early embryogenesis (43, 44).

Mxt is a functional analog of eIF4G. The relationship between Mxt and eIF4G is intriguing. eIF4G is the scaffold that promotes recruitment of the 40S ribosomal subunit to the mRNA 5′ end during cap-dependent translation (2, 4). eIF4G is a modular protein that in all species contains in the amino-terminal region binding sites for PABP and eIF4E. In mammalian eIF4Gs, the middle region contains a HEAT domain known as MIF4G that binds eIF4A, eIF3, and RNA, whereas the carboxy-terminal region, named MA3, includes two HEAT domains that possess a second binding site for eIF4A and W2, which binds the kinase Mnk (4). Mxt possesses an MIF4G at the amino-terminal end followed by a KH domain, a well-characterized RNA binding motif, and an eIF4E-binding site at the carboxy terminus. Thus, Mxt is a novel type of scaffolding protein that binds RNA, eIF3, and eIF4Es and promotes translation, as does eIF4G. Since Mxt contains MIF4G and KH domains, we consider it likely that Mxt binds to RNA

directly. In support of this, we found that Mxt was specifically recovered on poly(A)-Sepharose beads from lysates expressing Mxt-HA from a transfected plasmid (see Fig. S4 in the supplemental material). However, we cannot exclude that the Mxt-RNA interaction could be indirect and that RNase treatment could disrupt RNP complexes in which Mxt is present but not directly bound to RNA. How Mxt promotes translation without binding to eIF4A is also an intriguing open question. We speculate that either no helicase activity is required for Mxt-dependent translation or perhaps CG3225 can provide that activity in the absence of eIF4A.

The MIF4G domain is also present in other proteins involved in several processes of mRNA metabolism, such as Upf2/NMD2 and CBP80 (33, 34, 45, 46). All translation factors that carry the MIF4G domain are positive effectors of translation. This is the case for all eIF4Gs (33, 34, 46, 47), p97/DAP5/NAT-1 (48–51), poly(A)-binding protein-interacting protein 1 (Paip-1) (52), stem-loop binding protein-interacting protein 1 (SLIP-1) (53), and CBP80/20-dependent translation initiation factor (CTIF) (54). Here we have shown that this is also the case for Mxt. Interestingly, only MIF4G together with the eIF4E-binding site suffices for recruitment of eIF3 (and consequently the 40S ribosomal subunit) to mRNA, thus forming the functional core of eIF4G to drive cap-dependent translation (47, 55–57). Indeed, some eIF4Gs like those from yeast (*S. cerevisiae* and *Schizosaccharomyces pombe*) carry an eIF4E-binding site along with the MIF4G as the sole HEAT domain (46) (Fig. 1A). Thus, Mxt represents a novel type of protein possessing the minimal functional core needed for cap-dependent translation that is not related to eIF4G.

Different 4E-BPs arose independently in diverse taxonomic groups during eukaryotic evolution (7), and the MIF4G domain has spread to diverse proteins across eukaryotes (33, 34, 45, 46). Mxt represents a novel and unique example of evolutionary convergence of eIF4G function and extends the concept of the scaffolding protein during translation to proteins nonphylogenetically related to eIF4G.

Mxt may play a role in GSC maintenance. Mxt is expressed at high levels in ovarian GSCs and early-stage cystocytes. It interacts with eIF4E-1, and loss of *mxt* leads to reduction in GSC number, disorganization of germ line cells in germaria, and reduced fecundity in aged females, indicating a defect in GSC maintenance. This is consistent with the recent demonstration that GSC maintenance strongly depends on tight regulation of eIF4E-1 activity, as a functional reduction of eIF4E-1 in ovary GSCs prevents these cells from transforming into cancer stem cells without affecting their normal development or maintenance (39). While we have not directly demonstrated that Mxt is involved in translation *in vivo*, our results support the notion that eIF4E-1 forms a functional complex with Mxt that is critical for GSC maintenance. Additional lines of evidence show that translational control plays a crucial role in ovary GSC biology (58, 59).

Our observations lend experimental support to the hypothesis that gene regulation in pluripotent cells may preferentially involve noncanonical components of the translational machinery (60). Other variant translation initiation factors, including eIF4E-3 and eIF4G2, and several variant ribosomal proteins (RpS5b, RpS10a, RpS19b, and RpL22-like) have been identified in expression profiling studies of ovary and embryo GSCs and primordial germ cells (PGCs) (60, 61). Taken together with our results, these data indicate that the translational machinery in GSCs and PGCs may differ from that in somatic cells and that these differences may be fundamental to the biology of pluripotent cells.

ACKNOWLEDGMENTS

We are thankful to Paula Vázquez-Pianzola for plasmids and protocols, Gritta Tettweiler for protocols, Stanley Fields and the *Drosophila* Genomics Resource Center (DGRC) for plasmids, José Manuel Sierra, Matthias Hentze, Sandra Wolin, and Isabel Palacios for antibodies, Armen Parsyan, Bruno Fonseca, and Thomas Sundermeier for useful discussions, and Beili Hu for microinjections.

This work was supported by grant MOP-44050 to P.L. and N.S. from the Canadian Institutes of Health Research.

REFERENCES

1. **Kong J, Lasko P.** 2012. Translational control in cellular and developmental processes. Nat. Rev. Genet. **13:**383–394.
2. **Sonenberg N, Hinnebusch AG.** 2007. New modes of translation control in development, behavior, and disease. Mol. Cell **28:**721–729.
3. **Thompson B, Wickens M, Kimble J.** 2007. Translational control in development, p 507–544. *In* Mathews MB, Sonenberg N, Hershey JWB (ed), Translational control in biology and medicine. Cold Spring Harbor Laboratory Press, Cold Spring Harbor, NY.
4. **Jackson RJ, Hellen CU, Pestova TV.** 2010. The mechanism of eukaryotic translation initiation and principles of its regulation. Nat. Rev. Mol. Cell Biol. **11:**113–127.
5. **Sonenberg N, Hinnebusch A.** 2009. Regulation of translation initiation in eukaryotes: mechanisms and biological targets. Cell **136:**731–745.
6. **Richter JD, Sonenberg N.** 2005. Regulation of cap-dependent translation by eIF4E inhibitory proteins. Nature **433:**477–480.
7. **Hernández G, Altmann M, Lasko P.** 2010. Origins and evolution of the mechanisms regulating translation initiation in eukaryotes. Trends Biochem. Sci. **35:**63–73.
8. **Hernández G, Altmann M, Sierra JM, Urlaub H, Corral RD, Schwartz P, Rivera-Pomar R.** 2005. Functional analysis of seven genes encoding eight translation initiation factor 4E (eIF4E) isoforms in *Drosophila*. Mech. Dev. **122:**529–543.
9. **Cole C, Barber JD, Barton GJ.** 2008. The Jpred 3 secondary structure prediction server. Nucleic Acids Res. **36:**W197–W201.
10. **Söding J.** 2005. Protein homology detection by HMM-HMM comparison. Bioinformatics **21:**951–960.
11. **Altschul SF, Madden TL, Schäffer A, Zhang J, Zhang Z, Miller W, Lipman DJ.** 1997. Gapped BLAST and PSI-BLAST: a new generation of protein database search programs. Nucleic Acids Res. **25:**3389–3402.
12. **Pause A, Belsham GJ, Gingras A-C, Donzé O, Lin TA, Lawrence JC, Sonenberg N.** 1994. Insulin-dependent stimulation of protein synthesis by phosphorylation of a regulator of 5′-cap function. Nature **371:**762–767.
13. **Bischof J, Maeda RK, Hediger M, Karch F, Basler K.** 2007. An optimized transgenesis system for *Drosophila* using germ-line-specific phiC31 integrases. Proc. Natl. Acad. Sci. U. S. A. **104:**3312–3317.
14. **Cagney G, Uetz P, Fields S.** 2000. High-throughput screening for protein-protein interactions using two-hybrid assay. Methods Enzymol. **328:**3–17.
15. **Lachance PED, Miron M, Raught B, Sonenberg N, Lasko P.** 2002. Phosphorylation of eukaryotic translation initiation factor 4E is critical for growth. Mol. Cell. Biol. **22:**1656–1663.
16. **Zapata JM, Martinez MA, Sierra JM.** 1994. Purification and characterization of eukaryotic polypeptide chain initiation factor 4F from *Drosophila melanogaster* embryos. J. Biol. Chem. **269:**18047–18052.
17. **Duncan KE, Strein C, Hentze MW.** 2009. The SXL-UNR corepressor complex uses a PABP-mediated mechanism to inhibit ribosome recruitment to *msl-2* mRNA. Mol. Cell **36:**571–582.
18. **Palacios IM, Gatfield D, St Johnston D, Izaurralde E.** 2004. An eIF4AIII-containing complex required for mRNA localization and nonsense-mediated mRNA decay. Nature **427:**753–757.
19. **Roy G, Miron M, Khaleghpour K, Lasko P, Sonenberg N.** 2004. The *Drosophila* poly(A) binding protein-interacting protein, dPaip2, is a novel effector of cell growth. Mol. Cell. Biol. **24:**1143–1154.
20. **Miron M, Verdú J, Lachance PE, Birnbaum MJ, Lasko PF, Sonenberg N.** 2001. The translational inhibitor 4E-BP is an effector of PI(3)K/Akt signalling and cell growth in *Drosophila*. Nat. Cell Biol. **3:**596–601.

21. **Yoo CJ, Wolin SL.** 1994. La proteins from *Drosophila melanogaster* and *Saccharomyces cerevisiae*: a yeast homolog of the La autoantigen is dispensable for growth. Mol. Cell. Biol. **14:**5412–5424.
22. **Liu N, Han H, Lasko P.** 2009. Vasa promotes Drosophila germline stem cell differentiation by activating mei-P26 translation by directly interacting with a (U)-rich motif in its 3′ UTR. Genes Dev. **23:**2742–2752.
23. **Liu N, Dansereau DA, Lasko P.** 2003. Fat Facets interacts with Vasa in the *Drosophila* pole plasm and protects it from degradation. Curr. Biol. **13:** 1905–1909.
24. **Hughes S, Krause HM.** 1998. Single and double FISH protocols for *Drosophila*, p 50–65. *In* Paddock S (ed), Protocols in confocal microscopy. Humana Press, New York, NY.
25. **Gebauer F, Hentze MW.** 2007. Studying translational control in *Drosophila* cell-free systems. Methods Enzymol. **429:**23–33.
26. **Quiñones-Coello AT, Petrella LN, Ayers K, Melillo A, Mazzalupo S, Hudson AM, Wang S, Castiblanco C, Buszczak M, Hoskins RA, Cooley L.** 2007. Exploring strategies for protein trapping in *Drosophila*. Genetics **175:**1089–1104.
27. **Parks AL, Cook KR, Belvin M, Dompe NA, Fawcett R, Huppert K, Tan LR, Winter CG, Bogart KP, Deal JE, Deal-Herr ME, Grant D, Marcinko M, Miyazaki WY, Robertson S, Shaw KJ, Tabios M, Vysotskaia V, Zhao L, Andrade RS, Edgar KA, Howie E, Killpack K, Milash B, Norton A, Thao D, Whittaker K, Winner MA, Friedman L, Margolis J, Singer MA, Kopczynski C, Curtis D, Kaufman TC, Plowman GD, Duyk G, Francis-Lang HL.** 2004. Systematic generation of high-resolution deletion coverage of the *Drosophila melanogaster* genome. Nat. Genet. **36:**288–292.
28. **McKearin D, Ohlstein B.** 1995. A role for the *Drosophila bag-of-marbles* protein in the differentiation of cystoblasts from germline stem cells. Development **121:**2937–2947.
29. **Thibault ST, Singer MA, Miyazaki WY, Milash B, Dompe NA, Singh CM, Buchholz R, Demsky M, Fawcett R, Francis-Lang HL, Ryner L, Cheung LM, Chong A, Erickson C, Fisher WW, Greer K, Hartouni SR, Howie E, Jakkula L, Joo D, Killpack K, Laufer A, Mazzotta J, Smith RD, Stevens LM, Stuber C, Tan LR, Ventura R, Woo A, Zakrajsek I, Zhao L, Chen F, Swimmer C, Kopczynski C, Duyk G, Winberg ML, Margolis J.** 2004. A complementary transposon tool kit for *Drosophila melanogaster* using P and piggyBac. Nat. Genet. **36:**283–287.
30. **Alexandre C.** 2008. Cuticle preparation of Drosophila embryos and larvae. Methods Mol. Biol. **420:**197–205.
31. **Ausubel FM, Brent R, Kingston RE, Moore DD, Seidman JG, Smith JA, Struhl K.** 1998. Current protocols in molecular biology. John Wiley & Sons, New York, NY.
32. **Lasko P.** 2000. The *Drosophila melanogaster* genome: translational factors and RNA binding proteins. J. Cell Biol. **150:**F51–F56.
33. **Aravind L, Koonin EV.** 2000. Eukaryotic-specific domains in translation initiation factors: implications for translation regulation and evolution of the translation system. Genome Res. **10:**1172–1184.
34. **Ponting CP.** 2000. Novel eIF4G domain homologues linking mRNA translation with nonsense-mediated mRNA decay. Trends Biochem. Sci. **25:**423–426.
35. **Valverde R, Edwards L, Regan L.** 2008. Structure and function of KH domains. FEBS J. **275:**2712–2726.
36. **Giot L, Bader JS, Brouwer C, Chaudhari A, Kuang B, Li Y, Hao L, Ooi CE, Godwin B, Vitols E, Vijayadamodar G, Pochart PM, H, Welsh M, Kong Y, Zerhusen B, Malcolm R, Varrone Z, Collis A, Minto M, Burgess S, McDaniel L, Stimpson ES, F, Williams J, Neurath K, Ioime N, Agee M, Voss E, Furtak K, Renzulli R, Aanensen N, Carrolla S, Bickelhaupt E, Lazovatsky Y, DaSilva A, Zhong J, Stanyon CA, Finley RL, Jr, White KP, Braverman M, Jarvie T, Gold S, Leach M, Knight JS, Shimkets RA, McKenna MP, Chant J, Rothberg JM.** 2003. A protein interaction map of *Drosophila melanogaster*. Science **302:**1727–1736.
37. **Zhong W, Sternberg PW.** 2006. Genome-wide prediction of *C. elegans* genetic interactions. Science **311:**1481–1484.
38. **Veraksa A, Bauer A, Artavanis-Tsakonas S.** 2005. Analyzing protein complexes in *Drosophila* with tandem affinity purification-mass spectrometry. Dev. Dyn. **232:**827–834.
39. **Song Y, Lu B.** 2011. Regulation of cell growth by Notch signaling and its differential requirement in normal vs. tumor-forming stem cells in *Drosophila.* Genes Dev. **25:**2644–2658.
40. **Buszczak M, Paterno S, Lighthouse D, Bachman J, Planck J, Owen S, Skora AD, Nystul TG, Ohlstein B, Allen A, Wilhelm JE, Murphy TD, Levis RW, Matunis E, Srivali N, Hoskins RA, Spradling AC.** 2007. The Carnegie protein trap library: a versatile tool for *Drosophila* developmental studies. Genetics **175:**1505–1531.
41. **Hernández G, Han H, Gandin V, Fabian L, Ferreira T, Zuberek J, Sonenberg N, Brill J, Lasko P.** 2012. Eukaryotic initiation factor 4E-3 is essential for meiotic chromosome segregation, cytokinesis and male fertility in *Drosophila*. Development **139:**3211–3220.
42. **McKearin DM, Spradling AC.** 1990. *bag-of-marbles*: a *Drosophila* gene required to initiate both male and female gametogenesis. Genes Dev. **4:**2242–2251.
43. **Fraser AG, Kamath RS, Zipperlen P, Martinez-Campos M, Sohrmann M, Ahringer JA.** 2000. Functional genomic analysis of *C. elegans* chromosome I by systematic RNA interference. Nature **408:**325–330.
44. **Sonnichsen B, Koski LB, Walsh A, Marschall P, Neumann B, Brehm M, Alleaume AM, Artelt J, Bettencourt P, Cassin E, Hewitson M, Holz C, Khan M, Lazik S, Martin C, Nitzsche B, Ruer M, Stamford J, Winzi M, Heinkel R, Roder M, Finell J, Hantsch H, Jones SJ, Jones M, Piano F, Gunsalus KC, Oegema K, Gonczy P, Coulson A, Hyman AA, Echeverri CJ.** 2005. Full-genome RNAi profiling of early embryogenesis in *Caenorhabditis elegans*. Nature **434:**462–469.
45. **Hernández G.** 2009. On the origin of the cap-dependent initiation of translation in eukaryotes. Trends Biochem. Sci. **34:**166–175.
46. **Marintchev A, Wagner G.** 2005. eIF4G and CBP80 share a common origin and similar domain organization: implications for the structure and function of eIF4G. Biochemistry **44:**12265–12272.
47. **Marcotrigiano J, Lomakin IB, Sonenberg N, Pestova TV, Hellen CU, Burley SK.** 2001. A conserved HEAT domain within eIF4G directs assembly of the translation initiation machinery. Mol. Cell **7:**193–203.
48. **Henis-Korenblit S, Shani G, Sines T, Marash L, Shohat G, Kimchi A.** 2002. The caspase-cleaved DAP5 protein supports internal ribosome entry site-mediated translation of death proteins. Proc. Natl. Acad. Sci. U. S. A. **16:**5400–5405.
49. **Hundsdoerfer P, Thoma C, Hentze MW.** 2005. Eukaryotic translation initiation factor 4GI and p97 promote cellular internal ribosome entry sequence-driven translation. Proc. Natl. Acad. Sci. U. S. A. **102:**13421–13426.
50. **Lee SH, McCormick F.** 2006. p97/DAP5 is a ribosome-associated factor that facilitates protein synthesis and cell proliferation by modulating the synthesis of cell cycle proteins. EMBO J. **25:**4008–4019.
51. **Marash L, Liberman N, Henis-Korenblit S, Sivan G, Reem E, Elroy-Stein O, Kimchi A.** 2008. DAP5 promotes cap-independent translation of Bcl-2 and CDK1 to facilitate cell survival during mitosis. Mol. Cell **30:**447–459.
52. **Craig AW, Haghighat A, Yu AT, Sonenberg N.** 1998. Interaction of polyadenylate-binding protein with the eIF4G homologue PAIP enhances translation. Nature **392:**520–523.
53. **Cakmakci NG, Lerner RS, Wagner EJ, Zheng L, Marzluff WF.** 2008. SLIP1, a factor required for activation of histone mRNA translation by the stem-loop binding protein. Mol. Cell. Biol. **28:**1182–1194.
54. **Kim KM, Cho H, Choi K, Kim J, Kim BW, Ko YG, Jang SK, Kim YK.** 2009. A new MIF4G domain-containing protein, CTIF, directs nuclear cap-binding protein CBP80/20-dependent translation. Genes Dev. **23:** 2033–2045.
55. **De Gregorio E, Preiss T, Hentze MW.** 1998. Translational activation of uncapped mRNAs by the central part of human eIF4G is 5′ end dependent. RNA **4:**828–836.
56. **De Gregorio E, Preiss T, Hentze MW.** 1999. Translation driven by an eIF4G core domain *in vivo*. EMBO J. **18:**4865–4874.
57. **Morino S, Imataka H, Svitkin YV, Pestova TV, Sonenberg N.** 2000. Eukaryotic translation initiation factor 4E (eIF4E) binding site and the middle one-third of eIF4GI constitute the core domain for cap-dependent translation, and the C-terminal one-third functions as a modulatory region. Mol. Cell. Biol. **20:**468–477.
58. **Rangan P, DeGenaro M, Lehmann R.** 2008. Regulating gene expression in the *Drosophila* germ line. Cold Spring Harbor Symp. Quant. Biol. **73:**1–8.
59. **Shen R, Weng C, Yu J, Xie T.** 2009. eIF4A controls germline stem cell self-renewal by directly inhibiting BAM function in the *Drosophila* ovary. Proc. Natl. Acad. Sci. U. S. A. **106:**11623–11628.
60. **Kai T, Williams D, Spradling AC.** 2005. The expression profile of purified *Drosophila* germline stem cells. Dev. Biol. **283:**486–502.
61. **Shigenobu S, Kitadate Y, Noda C, Kobayashi S.** 2006. Molecular characterization of embryonic gonads by gene expression profiling in *Drosophila melanogaster*. Proc. Natl. Acad. Sci. U. S. A. **103:**13728–13733.
62. **Huynh JR, St Johnston D.** 2004. The origin of asymmetry: early polarisation of the Drosophila germline cyst and oocyte Curr. Biol. **14:**R438–R449.